

# What caused the onset of the 1997–1998 El Niño?

Geert Jan van Oldenborgh  
*KNMI, De Bilt, The Netherlands*

October 20, 1999

## Abstract

There has been intense debate about the causes of the 1997–1998 El Niño. One side sees the obvious intense westerly wind events as the main cause for the exceptional heating in summer 1997, the other emphasizes slower oceanic processes. We present a quantitative analysis of all factors contributing to the onset of this El Niño. Specifically, we decompose the NINO3 index in the HOPE OGCM at 1 June 1997 into contributions from the fluxes and initial state at six months' lead time. The initial state thermal anomalies contribute about 40% compared with an average year, and the wind stress about 50%. Compared with the previous year, in which no El Niño developed, the main difference is in the zonal wind stress. This contribution is concentrated at the time and place of the strong westerly wind events in December 1996, March and April 1997. As westerly wind events are difficult to predict, this limited the predictability of the onset of this El Niño.

## The Problem

The 1997–1998 El Niño was one of the strongest on record. Unfortunately, its onset was not predicted as well as had been hoped (Pearce, 1997; McPhaden, 1999). In spite of claims that an El Niño could be predicted a year in advance, most predictions (Stockdale et al., 1998; Ji et al., 1996; Schneider et al., 1999; Kleeman et al., 1995) only started to indicate a weak event six months ahead of time. One reason for this may be that El Niño depends not only on slow internal factors, but also on external noise in the form of weather events in the western Pacific.

The classical picture of El Niño (Bjerknes, 1966; Philander, 1990) explains the positive feedback that keeps such a large temperature anomaly in quasi-equilibrium for many months. During normal conditions the temperature difference between the ‘warm pool’ near Indonesia and the ‘cold tongue’ in the eastern equatorial Pacific causes a difference in sea-level pressure across the Pacific. This intensifies the trade winds, which in turn sustain the temperature difference by pushing warm surface water to the west and drawing cold water to the surface in the east. This positive feedback loop is kept in check by nonlinear effects. During an El Niño the same loop acts in reverse. The temperature difference is much smaller, the pressure almost equal, and the trade winds slackened or even reversed. The different wind forcing causes a deeper thermocline and reduced upwelling, which in turn sustain the warmer surface water in the eastern Pacific.

This picture leaves open the question how an El Niño event is triggered and terminated. A variety of mechanisms has been proposed. The coarse features of the system may be described as an unstable mode of the nonlinear coupled ocean-atmosphere system (Neelin, 1991; Neelin et al., 1998), either oscillatory or chaotic. A physical mechanism of this mode is the build-up of warm water in the western Pacific, which is released in an El Niño event (Wyrtki, 1975, 1985; Jin, 1997). The warm water is redistributed to the east in the form of equatorial Kelvin waves in the thermocline that move the edge of the ‘warm pool’ eastwards. The atmospheric convergence zone normally located over the western Pacific also moves eastward (Picaut et al., 1996), decreasing or reversing the trade winds to the west of it. The onset of an El Niño event is often phase-locked to the seasonal cycle, with the peak of an El Niño episode occurring around Christmas.

The decline of El Niño and the subsequent opposite phase (La Niña) that complete one oscillation are driven by a negative feedback loop. In this picture the physical mechanism is coastal reflections of equatorial long waves. The same westerly wind anomalies that generate downwelling Kelvin waves strengthening an El Niño also generate off-equatorial upwelling Rossby waves. These propagate to the west and reflect into upwelling Kelvin waves at the western coasts, which counteract the original heating. This delayed negative feedback in combination with the positive feedback described above may sustain oscillations (the ‘delayed oscillator theory’; Suarez and Schopf, 1988; Battisti and Hirst, 1989). However, the reflections have not been unequivocally observed (Kessler and McPhaden, 1995; Boulanger and Menkes, 1995; McPhaden, 1999).

In contrast to the self-sustaining oscillator theories described above, the observed strength of El Niño does not vary in a regular oscillation pattern (e.g., Burgers and Stephenson, 1999). This is probably not due to chaotic behavior (van der Vaart, 1998). It is, however, compatible with a damped oscillator driven by ‘noise’: random influences from outside the system (period  $47 \pm 6$  months, damping time  $18 \pm 6$  months and rms S/N ratio of the NINO3 index about 1.3; Burgers, 1999). A large part of this noise may be in the form of westerly wind events in the western Pacific, which are often associated with the onset of El Niño (Wyrтки, 1985; Kessler et al., 1995; Penland and Sardeshmukh, 1995; Flügel and Chang, 1996; Kleeman and Moore, 1997; Blanke et al., 1997; Eckert and Latif, 1997). The strong interannual variability of these wind events does not seem to be linked to El Niño (Slingo et al., 1999) and is currently unpredictable.

A detailed qualitative discussion of the visibility of the delayed oscillator mechanism and the influence of westerly wind events in the observations of the genesis and evolution of the 1997/98 El Niño can be found in McPhaden (1999).

In this paper we use a numerical ocean model and its derivative (adjoint model) to give a quantitative answer to the question how much the predictable slow ocean processes contributed to the strong onset of the El Niño in May 1997, and how much was due to unpredictable weather processes. We study these influences over the six preceding months, the time scale over which predictions are currently skillful. Although El Niño is an oscillation of the coupled ocean-atmosphere system, the analysis can be simplified by first studying the response of the ocean to forcing with observed wind stress and heat flux fields. This response contains all time delays, as the atmosphere reacts very quickly to changes in SST. The other part of the loop, the dependence of the wind stress and heat flux on the ocean surface temperature will be discussed qualitatively.

## The Model

The ocean model used is the Hamburg Ocean Primitive Equation Model, HOPE (Frey et al., 1997; Wolff et al., 1997) version 2.3, which is very similar to the ocean component of the European Centre for Medium-range Weather Forecasts (ECMWF) seasonal prediction system (Stockdale et al., 1998), but restricted to the Pacific Ocean. It is a general circulation model with a horizontal resolution of  $2.8^\circ$ , increased to  $0.5^\circ$  along the equator, and a vertical resolution of 25 m in

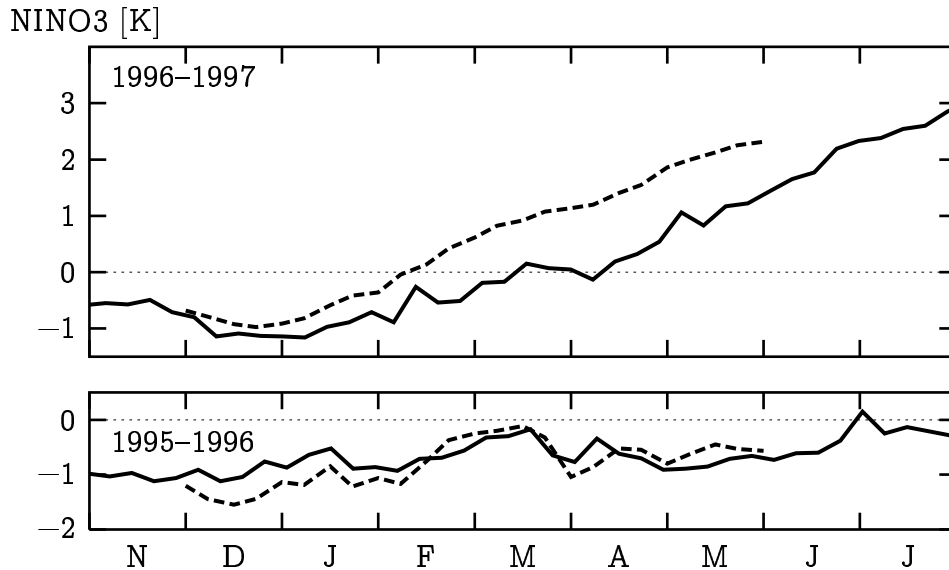


Figure 1: The NINO3 index observed (solid line) and simulated by the six-month forced model runs (dashed lines).

the upper ocean. It traces the evolution of temperature  $T$ , salinity  $S$ , horizontal velocities  $u, v$  and sea level  $\zeta$ .

This ocean model is forced with daily wind stress  $(\tau_x, \tau_y)$  and heat flux  $Q$  from the ECMWF analysis, which in turn uses the excellent system of buoys (McPhaden et al., 1997) that observed this El Niño. Evaporation and precipitation are only implemented as a relaxation to climatological surface salinity. The initial state conditions are ECMWF analyzed ocean states. To suppress systematic model errors we subtract a run starting from an average 1 December ocean state forced with 1979–1996 average wind and heat fluxes (ERA, Gibson et al., 1997).

The model simulates the onset of the 1997–1998 El Niño quite well. As a measure of the strength of El Niño we use the NINO3 index  $N_3$ , defined as the anomalous sea surface temperature in the area  $5^\circ\text{S}$ – $5^\circ\text{N}$ ,  $90^\circ\text{W}$ – $150^\circ\text{W}$ . In Fig. 1 the weekly observed NINO3 index (Reynolds and Smith, 1994) is shown together with the modeled value, both for 1996–1997 and one year earlier. The model overreacts somewhat to the forcing and simulates a NINO3 index of 2.3 K at 1 June 1997, whereas in reality the index reached this value one month later. In 1995–1996 the simulation follows reality very well.

## The Adjoint Model

The value of the NINO3 index at the end of a model run can be traced back to the model input (initial state, forcing) with an *adjoint model*. The normal ocean model is a (complicated) function  $\mathcal{M}$  that takes as input the state of the ocean at some time  $t_0$  (temperature  $T_0$ , salinity  $S_0$ , etc.). Using the wind stress  $\vec{\tau}_i$  and heat flux  $Q_i$  for each day  $i$  for six months it then produces a final state temperature  $T_n$ . The adjoint model (or backward derivative model) is the related function that takes as input derivatives to a scalar function of the final state, here the NINO3 index. This field  $\partial N_3 / \partial T_n$  is a constant at the surface in the NINO3 region and zero everywhere else. The adjoint model then goes backward in time and uses the chain rule of differentiation (Giering and Kaminski, 1998) to compute from these the derivatives  $\partial N_3 / \partial T_0$ ,  $\partial N_3 / \partial S_0$ ,  $\partial N_3 / \partial \vec{\tau}_i$  and  $\partial N_3 / \partial Q_i$ , using information from the forward simulation for nonlinear terms. These derivatives can be interpreted as *sensitivity fields*, giving the effect of a perturbation in the initial state or forcing fields on the NINO3 index at the end of the simulation:

$$\begin{aligned} \delta N_3 \approx & \frac{\partial N_3}{\partial T_0} \cdot \delta T_0 + \frac{\partial N_3}{\partial S_0} \cdot \delta S_0 \\ & + \sum_{\text{days } i} \left( \frac{\partial N_3}{\partial \vec{\tau}_i} \cdot \delta \vec{\tau}_i + \frac{\partial N_3}{\partial Q_i} \cdot \delta Q_i \right). \end{aligned} \quad (1)$$

The inner products denote integrals of the product of the fields. We have checked with actual perturbations that the accuracy of the linear approximation Eq. 1 is usually better than about 30% for realistic zonal wind stress anomalies (within the model). Details can be found in van Oldenborgh et al. (1999).

Now we specialize this equation to explain the difference between the simulation and the climatological run. In this case the left-hand side is just the NINO3 index  $N_3$ . The corresponding perturbations in the initial state and forcing fields are the anomalies with respect to climatology from the ERA (Gibson et al., 1997) and later operational ECMWF analyses. To minimize higher order terms we take for the sensitivities the average derivatives from the simulation and the climatology run. The result is a linear Taylor expansion of the NINO3 index with suppressed quadratic terms,

$$\begin{aligned} N_3^{\text{sim}} \approx & \frac{1}{2} \left( \frac{\partial N_3}{\partial T_0} \Big|_{\text{sim}} + \frac{\partial N_3}{\partial T_0} \Big|_{\text{clim}} \right) \cdot (T_0^{\text{sim}} - T_0^{\text{clim}}) \\ & + \frac{1}{2} \left( \frac{\partial N_3}{\partial S_0} \Big|_{\text{sim}} + \frac{\partial N_3}{\partial S_0} \Big|_{\text{clim}} \right) \cdot (S_0^{\text{sim}} - S_0^{\text{clim}}) \end{aligned}$$

$$\begin{aligned}
& + \sum_{\text{days } i} \frac{1}{2} \left( \left. \frac{\partial N_3}{\partial \bar{\tau}_i} \right|_{\text{sim}} + \left. \frac{\partial N_3}{\partial \bar{\tau}_i} \right|_{\text{clim}} \right) \cdot (\bar{\tau}_i^{\text{sim}} - \bar{\tau}_i^{\text{clim}}) \\
& + \sum_{\text{days } i} \frac{1}{2} \left( \left. \frac{\partial N_3}{\partial Q_i} \right|_{\text{sim}} + \left. \frac{\partial N_3}{\partial Q_i} \right|_{\text{clim}} \right) \cdot (Q_i^{\text{sim}} - Q_i^{\text{clim}}) . \quad (2)
\end{aligned}$$

This means that the value of the index is explained as a sum of the influences of initial state temperature and salinity, and the wind and heat forcing during the six months of the run.

## The onset of the 1997–1998 El Niño

For the value of the NINO3 index on 1 June 1997 the expansion Eq. 2 gives a value of 1.8 K, compared with the 2.3 K simulated (and 1.3 K observed), this is within the expected error. The high value is mainly due to the influence of the westerly wind anomalies, 1.0 K, and the initial state temperature on 1 December 1996, 1.1 K. The salinity contributes  $-0.3$  K, with a large uncertainty due to the relaxation to climatology. The remaining terms, heat flux and meridional wind stress, are less than 0.1 K.

The spatial structure of the influence of the initial state temperature is shown in Fig. 2. The top panel gives the temperature anomaly  $\delta T_0$  superimposed on the temperature  $T_0$  along the equator at the beginning of the run (Dec 1996), showing an unusually deep thermocline in the western Pacific and a shallower thermocline in the eastern Pacific. The second frame depicts the sensitivity of the June NINO3 index to temperature anomalies six months earlier,  $\partial N_3 / \partial T_0$ . The third frame is just the product of the previous two; the integral of this over the whole ocean gives the 1.1 K contribution to the NINO3 index mentioned before. The contribution is concentrated in the deeper layer of warm water along the equator in the western Pacific, in agreement with a ‘recharge’ mechanism.

To study the influence of the wind stress in more detail we have rewritten the third term of the right hand side of Eq. 2 as a sum of contributions from the different weeks of the six-month simulation. These are shown in Fig. 3 (solid line). The area under the graph is the sum of the weekly contributions of zonal wind stress to the June NINO3 anomaly, 1.0 K. One sees that the positive contributions are concentrated in two periods, the month of March and the beginning of April. These coincide with three peaks in a measure of the zonal wind stress in the western Pacific (dashed line). These peaks correspond with

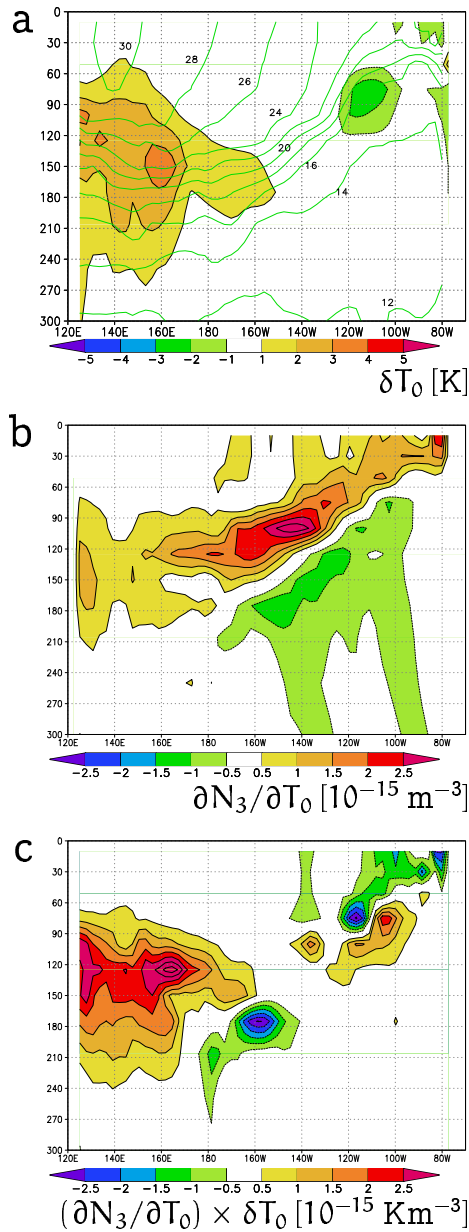


Figure 2: Depth-longitude plots of the effect of the initial state temperature on the NINO3 index in early June. At the top the analyzed temperature anomalies at the beginning of December 1996 are shown (contours: analyzed temperatures); the second frame depicts the sensitivity of the ocean to these temperature anomalies and the third the product of these two, which gives the rise in the NINO3 index on June 1 due to the thermal structure six months earlier. All quantities are averaged over 5°S–5°N.

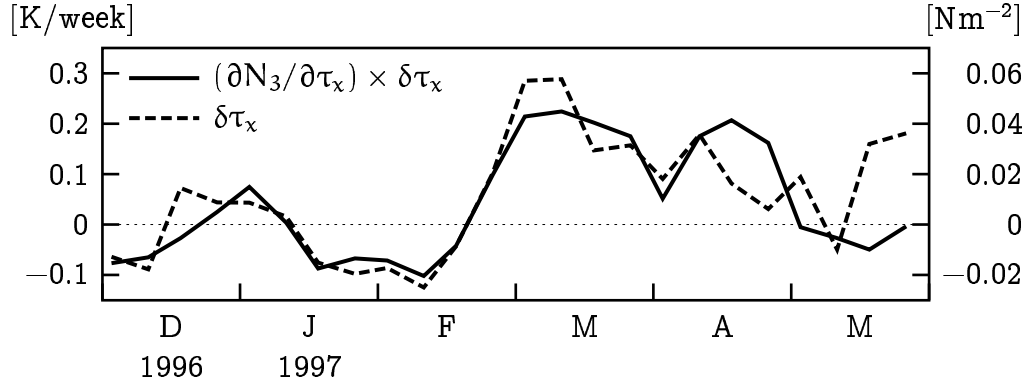


Figure 3: The influence of the zonal wind stress  $\tau_x$  on the NINO3 index at 1 June 1997 during the previous six months (solid line), the average anomalous wind stress over the area  $130^\circ\text{E}$  to  $160^\circ\text{W}$ ,  $5^\circ\text{S}$  to  $5^\circ\text{N}$ .

(very) strong westerly wind events in this area. These generated dips in the thermocline that traveled east as Kelvin waves and deepened the layer of warm water in the eastern Pacific 2–3 months later, increasing the surface temperature by about 0.6 K, 0.3 K and 0.5 K respectively. Note that the strong trade winds before the end of February had given a negative contribution of  $-0.4$  K.

There was also a strong wind event in December, contributing about 0.4 K over a negative baseline. From Fig. 3 it seems likely that it increased the strength of the later wind events by heating the eastern Pacific in March: the baseline of the zonal wind stress anomalies seems to have increased from around  $-0.02 \text{ Nm}^{-2}$  before March to zero afterwards. The heating effect of the March wind event also gave rise to an increase of the wind stress  $\delta\tau_x$  in May, but this reversal of the trade winds does not yet influence the NINO3 index  $\partial N_3/\partial\tau_x \cdot \delta\tau_x$ , justifying the uncoupled analysis.

The structure of the peaks in Fig. 3 can be seen more clearly in spatial views. In Fig. 4a the zonal wind stress anomaly  $\delta\tau_x$  is plotted for the second week of March. The westerly wind event corresponds to the large localized westerly anomaly around  $150^\circ\text{E}$ . Fig. 4b shows the sensitivity of the NINO3 index in June to the zonal wind stress during this week,  $\partial N_3/\partial\tau_x$ . This sensitivity consists of two main parts, both equatorally confined. In the western Pacific extra westerly wind stress would excite downwelling Kelvin waves, depressing the thermocline in the eastern Pacific two months later and raising the NINO3 index on June 1. In the eastern equatorial Pacific the response to a wind stress anomaly would be in the form of Rossby waves that propagate to the edges of the NINO3 region. In this region the validity of the linearization Eq. 1 is

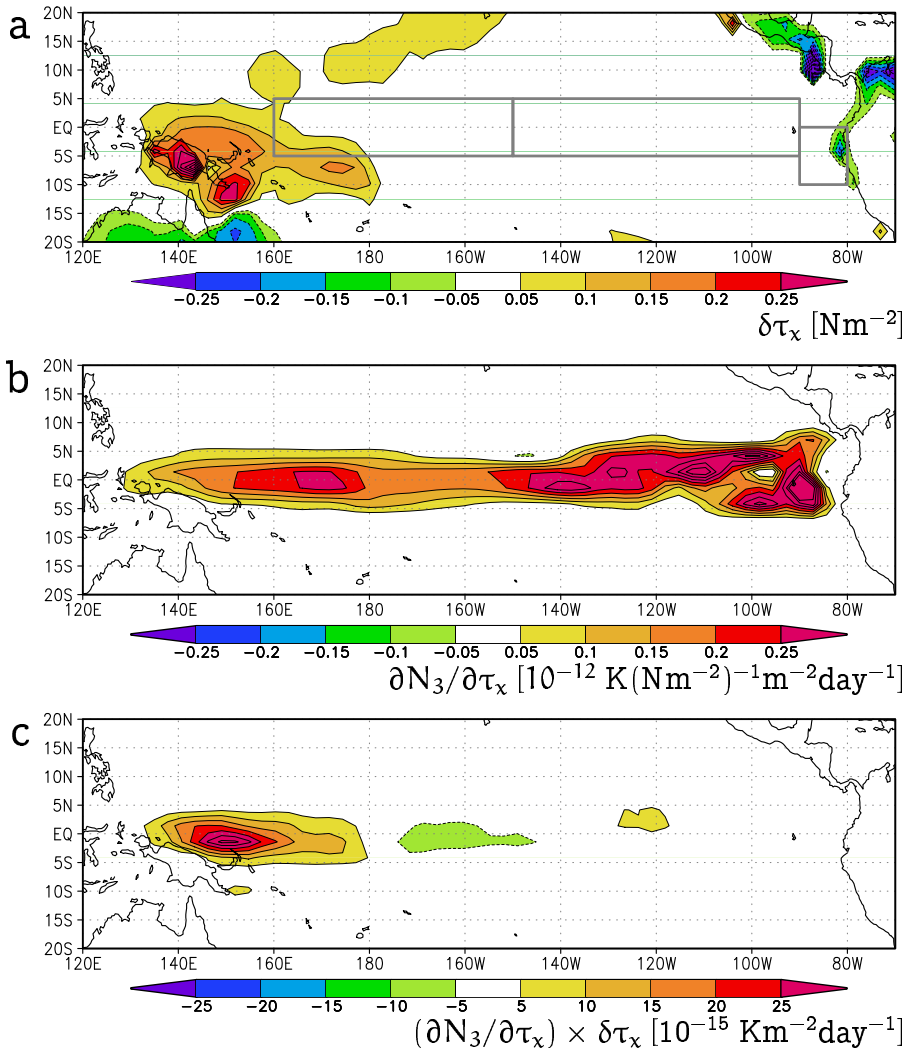


Figure 4: The effect of the March westerly wind event on the NINO3 index in early June. At the top the averaged westerly wind stress anomaly for the week centered on 11 March 1997 is shown, the second frame depicts the sensitivity of the ocean to zonal wind stress and the third the product of these two which gives the rise in the NINO3 index on June 1 due to this wind event.

doubtful.

The product of the anomaly and sensitivity fields is shown in Fig. 4c. This gives the influence of zonal wind stress during this week on the NINO3 index, the integral of this field gives the corresponding value (0.22 K) in Fig. 3. The influence is contained in the intersection of the westerly wind event and the equatorial wave guide, and very localized in time and space. The unreliable high sensitivities in the eastern Pacific do not contribute. The contributions from the other wind events have similar structures.

These findings agree with the qualitative analysis of McPhaden (1999), who also finds a contribution from the build-up of heat content in the western Pacific and attributes the sudden onset and large amplitude of the event at least in part to the westerly wind events (McPhaden and Yu, 1999). There are also broad similarities with the ‘stochastic optimals’ found by Moore and Kleeman (1999) in an intermediate coupled model.

## A comparison with 1996

The question remains whether the big influence of these wind events was due to their strength  $\delta\tau_x$  or to an increased sensitivity of the ocean  $\partial N_3/\partial\tau_x$ . We therefore repeated the analysis for the same months one year earlier, when the temperature in the eastern Pacific stayed below normal (Fig. 1). The adjoint model gives a NINO3 index of  $-0.6$  K, equal to the simulated index (the observed index was  $-0.7$  K). This index is built up by a large negative influence of the wind stress,  $-1.5$  K, and a positive influence of the heat flux,  $+0.9$  K. The influence of the initial state temperature is also positive, but weaker than in the 1996–1997 simulation,  $+0.6$  K. The salinity anomalies contributed  $-0.5$  K.

Although the build-up of warm water is also less pronounced, the largest difference is in the influence of the zonal wind stress. The sensitivity to zonal wind stress  $\partial N_3/\partial\tau_x$  (over the area where its variability is largest) is compared for these two years in Fig. 5. The sensitivities had the same order of magnitude in 1996 and 1997, particularly at the time of the strong early March 1997 wind event. In April 1997 the sensitivity was somewhat higher than in April 1996 and in December 1998 and January 1997 it was somewhat lower than the year before, but, in all, these differences cannot explain more than a few tenths of a degree difference in the NINO3 index on 1 June.

We can quantify the difference between an El Niño in June 1997 and no El Niño in June 1996 by using Eq. 2 to expand the difference in NINO3

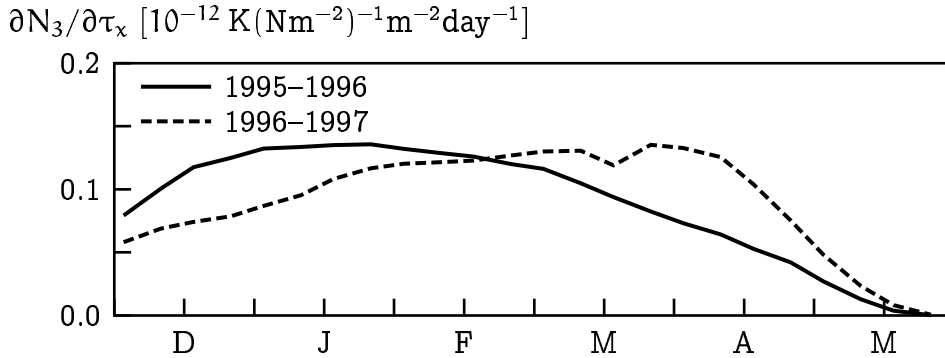


Figure 5: The average sensitivity of the NINO3 index on 1 June to westerly winds in the area defined in Fig. 3.

index at those times, rather than the difference with climatology. To linear order this is just the difference between the expansions of the two indices. The results are a simulated difference of 2.9 K (observed 2.0 K), of which the Taylor expansion explains 2.5 K as follows: initial state temperature 0.5 K (probably underestimated, see below), salinity 0.2 K (again with a large uncertainty), zonal wind stress 2.5 K, meridional wind stress 0.3 K and heat flux  $-1.0$  K. The adjoint model therefore attributes the difference between the two years for about 20% to an even stronger build-up of warm water in the western Pacific, and for about 100% to the zonal wind stress. This latter contribution is mainly due to the absence of strong westerly wind events in the western Pacific in the 1995–1996 season, although about 10% is caused by an easterly wind anomaly in early February 1996. The remaining (negative) influence is largely made up by the heat flux: the warmer water in 1997 cooled more. These results are somewhat more reliable than the numbers given before, as some of the model errors will have canceled in the comparison.

The accuracy of the linear approximation of Eq. 2 and the adjoint model has been checked by two simple crossing experiments. The ocean model was run using the ocean state of 1 December 1995 with the 1996–1997 fluxes, and using the 1 December 1996 analysis with the 1995–1996 fluxes. Assuming nonlinearities are small, the predictions from the Taylor expansion are easily found by recombining the terms from the 1995–1996 and 1996–1997 experiments. This gives  $N_3^{\text{adj}} = 1.1$  K and 0.0 K respectively. The results of the simulations are shown in Fig. 6. The simulated NINO3 indices at the end of the runs are 1.1 K and 1.0 K. From the discrepancy in the second case one can infer that the linearizations of the adjoint model tend to underestimate the influence of the

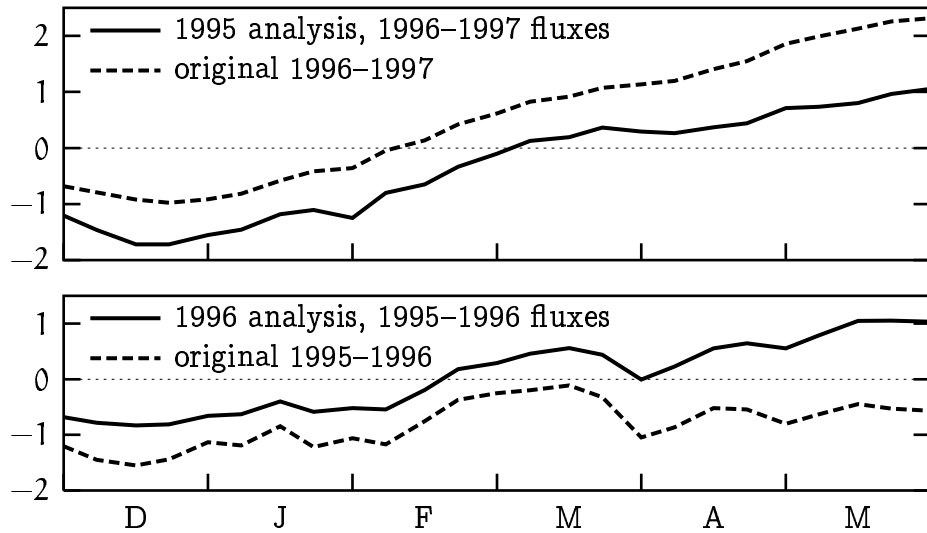


Figure 6: Two crossed simulations: the ocean state of 1 December 1995 with the 1996–1997 fluxes (top), and the 1 December 1996 analysis with the 1995–1996 fluxes (bottom). The dashed lines are the original simulations.

initial state.

## Conclusions

Using an adjoint ocean general circulation model we have investigated the causes of the strong onset of the 1997–1998 El Niño, compared with the absence of El Niño one year earlier. The adjoint model gives derivatives of the NINO3 index at the end of a simulation to the initial state and forcing fields. Multiplying with the anomalies of these fields we obtain the linear terms of a Taylor expansion of the NINO3 index. The largest term is the reaction to the strong westerly wind events in March–April 1997. In our model these contributed about 50% to the value of the NINO3 index on 1 June 1997. Comparing with the year before, when no El Niño occurred, the effect of these localized westerlies explains 90% of the difference. The sensitivity of the NINO3 index to these wind events was not significantly different from the year before, so the main cause of the effect was their strength.

The other significant positive factor was the build-up of warm water in the western Pacific, which explains 40% of the value of the NINO3 index on

1 June 1997 at a lead time of six months. This number is probably underestimated due to the linear approximation. In 1996 the warm pool was also deeper than normal, so that only 20% of the difference between 1996 and 1997 can be attributed to the different temperature distribution in December. The balance is made up by extra cooling of the warmer surface water in 1997 (−40%), plus small contributions from an easterly wind anomaly in February 1996, the meridional wind stress and salinity (about 10% each).

Within this model, a successful prediction of the strong onset of the 1997–1998 El Niño would have required a successful prediction of the strong wind events in 1996–1997, compared to a much less active season one year earlier. However, the year-to-year variability of these wind events does not seem to depend on the state of the Pacific ocean (Slingo et al., 1999), and at the moment is not predictable. This could explain the relatively short lead time for correct predictions of the strong onset of this El Niño.

*Acknowledgments* I would like to thank the ECMWF seasonal prediction group for their help and support, Gerrit Burgers for his part in the construction of the adjoint model and Gerbrand Komen for his suggestions for improving the presentation. This research was supported by the Netherlands Organization for Scientific Research (NWO).

## References

- Battisti, D. S. and A. C. Hirst, 1989: Interannual variability in a tropical atmosphere–ocean model: Influence of the basic state, ocean geometry and nonlinearity. *J. Atmos. Sci.*, **46**, 1687–1712.
- Bjerknes, J., 1966: A possible response of the atmospheric Hadley circulation to equatorial anomalies of ocean temperature. *Tellus*, **18**, 820–829.
- Blanke, B., J. D. Neelin, and D. Gutzler, 1997: Estimating the effect of stochastic wind forcing on ENSO irregularity. *J. Climate*, **10**, 1473–1486.
- Boulangier, J.-P. and C. Menkes, 1995: Propagation and reflection of long equatorial waves in the Pacific ocean during the 1992–1993 El Niño. *J. Geophys. Res.*, **100**, 25041–25059.
- Burgers, G., 1999: The El Niño stochastic oscillator. *Climate Dynamics*, **15**, 521–531.
- Burgers, G. and D. B. Stephenson, 1999: The normality of El Niño. *Geophys. Res. Lett.*, **26**, 1027–1030.

- Eckert, C. and M. Latif, 1997: Predictability of a stochastically forced hybrid coupled model of ENSO. *J. Climate*, **10**, 1488–1504.
- Flügel, M. and P. Chang, 1996: Impact of dynamical and stochastic processes on the predictability of ENSO. *Geophys. Res. Lett.*, **23**, 2089–2092.
- Frey, H., M. Latif, and T. Stockdale, 1997: The coupled GCM ECHO-2. Part I: The tropical Pacific. *Mon. Wea. Rev.*, **125**, 703–720.
- Gibson, R., P. Källberg, S. Uppala, A. Hernandez, A. Nomura, and E. Serrano, 1997: ECMWF re-analysis 1. ERA description. Technical report, ECMWF, Reading, UK.
- Giering, R. and T. Kaminski, 1998: Recipes for adjoint code construction. *ACM Trans. Math. Software*, **24**, 437–474.
- Ji, M., A. Leetmaa, and V. E. Kousky, 1996: Coupled model predictions of ENSO during the 1980s and 1990s at the National Centers for Environmental Prediction. *J. Clim.*, **9**, 3105–3120. Forecasts are under <http://nic.fb4.noaa.gov>.
- Jin, F.-F., 1997: An equatorial recharge paradigm for ENSO, part I: Conceptual model. *J. Atmos. Sci.*, **54**, 811–829.
- Kessler, W. S. and M. J. McPhaden, 1995: Oceanic equatorial waves and the 1991–93 El Niño. *J. Climate*, **8**, 1757–1774.
- Kessler, W. S., M. J. McPhaden, and K. M. Weickman, 1995: Forcing of intraseasonal Kelvin waves in the equatorial Pacific. *J. Geophys. Res.*, **100**, 10613–10631.
- Kleeman, R., A. Moore, and N. R. Smith, 1995: Assimilation of subsurface thermal data into a simple ocean model for the initialization of an intermediate tropical coupled ocean–atmosphere forecast model. *Mon. Wea. Rev.*, **123**, 3103–3114. Forecasts are at <http://www.bom.gov.au/bmrc/mrlr/rzk/climfcn3.htm>.
- Kleeman, R. and A. M. Moore, 1997: A theory for the limitations of ENSO predictability due to stochastic atmospheric transients. *J. Atmos. Sci.*, **54**, 753–767.
- McPhaden, M. J., 1999: Genesis and evolution of the 1997–98 El Niño. *Science*, **283**, 950–954.
- McPhaden, M. J., A. J. Busalacchi, R. Cheney, J. R. Donguy, K. S. Gage, D. Halpern, M. Ji, P. Julian, G. Meyers, G. T. Mitchum, P. P. Niiler, J. Picaut, R. W. Reynolds, N. Smith, and K. Takeuchi, 1997: The Tropical Ocean Global Atmosphere (TOGA) observing system: a decade of progress. *J. Geophys. Res.*, **100**, 14169.

- McPhaden, M. J. and X. Yu, 1999: Equatorial waves and the 1997–1998 El Niño. *Geophys. Res. Lett.*, **26**, 2961–2964.
- Moore, A. M. and R. Kleeman, 1999: Stochastic forcing of ENSO by the intraseasonal oscillation. *J. Climate*, **12**, 1199–1220.
- Neelin, J. D., 1991: The slow sea-surface temperature mode and the fast-wave limit: Analytic theory for tropical interannual oscillations and experiments in a hybrid coupled model. *J. Atmos. Sci.*, **48**, 584–606.
- Neelin, J. D., D. S. Battisti, A. C. Hirst, F.-F. Jin, Y. Wakata, T. Yamagata, and S.E. Zebiak, 1998: ENSO theory. *J. Geophys. Res.*, **103**, 14261–14290.
- Pearce, F., 1997: Sneaky El Niño outwits weather forecasters. *New Scientist*, **31** May, 6.
- Penland, C. and P. D. Sardeshmukh, 1995: The optimal growth of tropical sea surface anomalies. *J. Climate*, **8**, 1999–2024.
- Philander, S. G., 1990: *El Niño, La Niña and the Southern Oscillation*. Academic Press, 293 pp.
- Picaut, J., M. Ioulalen, C. Menkes, and T. Delcroix, 1996: Mechanism of the zonal displacement of the Pacific warm pool: implications for ENSO. *Science*, **274**, 1486–1489.
- Reynolds, R. W. and T. M. Smith, 1994: Improved global sea surface analyses using optimum interpolation. *J. Clim.*, **7**, 929–948. NINO indices are available from the Climate Prediction Center at <http://nic.fb4.noaa.gov/data/cddb/altindex.html>.
- Schneider, E. K., B. Huang, Z. Zhu, D. G. DeWitt, J. L. Kinter III, B. Kirtman, and J. Shukla, 1999: Ocean data assimilation, initialization, and predictions of ENSO with a coupled GCM. *Mon. Wea. Rev.*, **127**, 1187–1207. Forecasts are published at <http://www.iges.org/ellfb>.
- Slingo, J. M., D. P. Rowell, K. R. Sperber, and F. Nortley, 1999: On the predictability of the interannual behaviour of the Madden-Julian Oscillation and its relationship with El Niño. *Quart. J. Roy. Meteorol. Soc.*, **125**, 583–608.
- Stockdale, T. N., D. L. T. Anderson, J. O. S. Alves, and M. A. Balmaseda, 1998: Global seasonal rainfall forecasts using a coupled ocean–atmosphere model. *Nature*, **392**, 370–373.
- Suarez, M. J. and P. S. Schopf, 1988: A delayed action oscillator for ENSO. *J. Atmos. Sci.*, **45**, 3283–3287.
- van der Vaart, P. C. F., 1998: *Nonlinear tropical climate dynamics*. PhD thesis, Universiteit Utrecht.
- van Oldenborgh, G. J., G. Burgers, S. Venzke, C. Eckert, and R. Giering, 1999:

- Tracking down the ENSO delayed oscillator with an adjoint OGCM. *Mon. Wea. Rev.*, **127**, 1477–1496.
- Wolff, J.-O., E. Maier-Reimer, and S. Legutke, 1997: The Hamburg Ocean Primitive Equation model HOPE. Technical Report No. 13, Deutsches Klimarechenzentrum, Bundesstr. 55, D-20146 Hamburg, Germany, Hamburg.
- Wyrтки, K., 1975: El Niño — the dynamic response of the equatorial Pacific Ocean to atmospheric forcing. *J. Phys. Oceanogr.*, **5**, 572–584.
- Wyrтки, K., 1985: Water displacements in the Pacific and the genesis of El Niño. *J. Geophys. Res.*, **90**, 7129–7132.